

Cite this: *Chem. Soc. Rev.*, 2011, **40**, 2120–2130

www.rsc.org/csr

## TUTORIAL REVIEW

**Zebrafish as a good vertebrate model for molecular imaging using fluorescent probes**Sung-Kyun Ko,<sup>a</sup> Xiaoqiang Chen,<sup>bc</sup> Juyoung Yoon\*<sup>b</sup> and Injae Shin\*<sup>a</sup>

Received 22nd September 2010

DOI: 10.1039/c0cs00118j

Fluorescent probes have been used extensively to monitor biomolecules and biologically relevant species *in vitro* and *in vivo*. A new trend in this area that has been stimulated by the desire to obtain more detailed information about the biological effects of analytes is the change from live cell to whole animal fluorescent imaging. Zebrafish has received great attention for live vertebrate imaging due to several noticeable advantages. In this *tutorial review*, recent advances in live zebrafish imaging using fluorescent probes, such as fluorescent proteins, synthetic fluorescent dyes and quantum dots, are highlighted.

**1. Introduction**

Molecular imaging technologies enable visualization of (bio)molecules and ions in cells, tissues and organisms with the aim of gaining information about the biological effects of the analytes. Fluorescent probes, such as synthetic organic dyes, fluorescent proteins and quantum dots, have become popular tools for molecular imaging owing to their high sensitivity, simple manipulation and the lack of a need for

sophisticated instrumentation.<sup>1–8</sup> In particular, fluorescent probes that respond to analytes with high selectivity and sensitivity have been widely employed to monitor biomolecules and biologically relevant species as well as to probe biological events in a spatio-temporal manner. In many cases, molecular imaging using fluorescent probes has been carried out within cells. However, live cell imaging is not totally acceptable for obtaining detailed information about the biological effects of analytes. In contrast, images of the insides of live animals provide a more informative view of these effects. Moreover, fluorescent imaging studies using organisms that are genetically close to humans have become highly attractive (Fig. 1).

Mouse is a good animal model, but its manipulation and *in vivo* whole animal imaging require special techniques and complex manipulations. In contrast, zebrafish (*Danio rerio*) has proved to be a highly valuable vertebrate model for *in vivo* imaging in a variety of biological investigations.<sup>9</sup> In fact, zebrafish has several noteworthy advantages for live animal imaging. Firstly, both adult and young zebrafish can be easily

<sup>a</sup> Center for Biofunctional Molecules, Department of Chemistry, Yonsei University, Seoul 120-749, Korea.  
E-mail: injae@yonsei.ac.kr; Fax: +82 2364-7050;  
Tel: +82 2-2123-2631

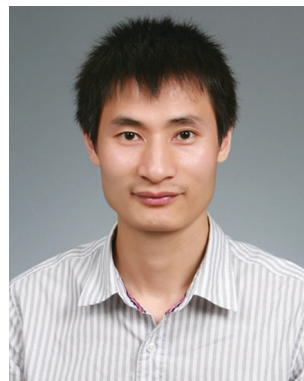
<sup>b</sup> Department of Chemistry and Nano Science and Department of Bioinspired Science, Ewha Womans University, Seoul 120-750, Korea. E-mail: jyoon@ewha.ac.kr; Fax: +82 2-3277-2384;  
Tel: +82 2-3277-2400

<sup>c</sup> State Key Laboratory of Materials-Oriented Chemical Engineering, College of Chemistry and Chemical Engineering, Nanjing University of Technology, Nanjing 210009, China



Sung-kyun Ko

Sung-kyun Ko was born in Seoul, South Korea, in 1977. He received his BS degree in Biotechnology in 2002 from Daegu University. His MS degree was awarded in 2004 in Molecular Biology at the Sejong University. He began his Ph.D. with Professor Injae Shin at Yonsei University in 2006. His current research interests include screening of bioactive molecules and their biological studies as well as *in vivo* imaging of (bio)molecules.



Xiaoqiang Chen

Xiaoqiang Chen was born in China, in 1980. He received his PhD in Applied Chemistry from Dalian University of Technology (China) in 2007. In 2008 he joined Professor Yoon's group at Ewha Womans University (Korea) as a post-doctoral fellow. Since March 2010 he has been faculty at Nanjing University of Technology. His current research interests mainly focus on fluorescent chemosensors.

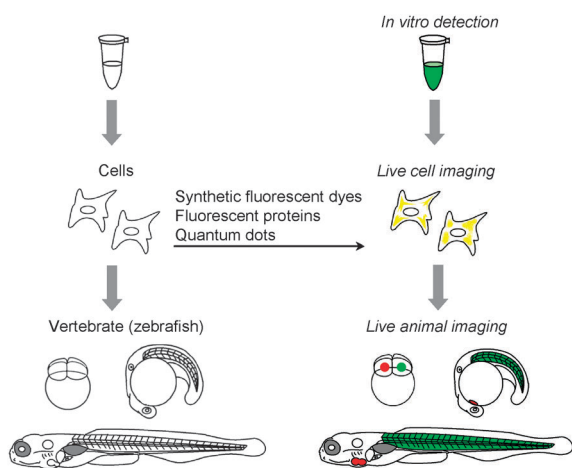


**Fig. 1** Live cell and animal imaging using fluorescent probes. The trend for detection of analytes has changed from live cell imaging to whole animal imaging.

maintained for imaging applications. Secondly, zebrafish is optically transparent during early development and, as a result, optical imaging techniques can be readily used. Thirdly, zebrafish fertilization is external, which enables live animal imaging during all stages of embryonic development. Finally, zebrafish has high homology with mammals. Owing to this feature, the results obtained from the use of this organism can be used to model biological effects of analytes that occur in higher animals. However, care should be taken when extrapolating results obtained from zebrafish studies to mammals since fundamental functional processes differ between two species in some cases. For example, fish ventilation and respiratory function are different from mammals albeit their genetic similarities.

In efforts aimed at monitoring analytes and probing biological consequences in vertebrates, numerous fluorescent imaging studies have been performed using zebrafish. The results of investigations discussed in this review show that

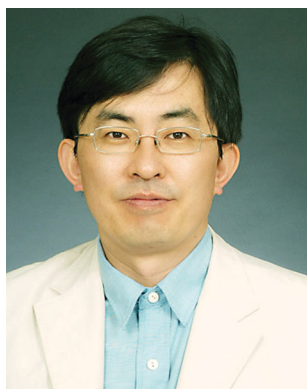
zebrafish holds great potential in live animal imaging. To demonstrate this point, we first discuss fluorescent proteins and recent advances made in zebrafish imaging using these proteins. Advances in monitoring biomolecules and biologically relevant species in zebrafish using synthetic fluorescent probes will then be reviewed. In addition, we discuss zebrafish imaging using quantum dots, which have been recently developed as *in vitro* and *in vivo* fluorophores for various biological studies. Finally, the review concludes with a discussion of the perspectives of fluorescent probe development and potential applications for the zebrafish imaging.

## 2. Zebrafish imaging using fluorescent proteins

### 2.1 Fluorescent proteins

Since the discovery of the green fluorescent protein (GFP) from the jellyfish *Aequorea victoria*, fluorescent proteins have become an indispensable tool for the visualization and study of complex biological phenomena in cells and animals. To date, more than thirty different fluorescent protein family members have been produced<sup>10</sup> and employed as genetically encodable fusion reporters in investigations of protein localization and dynamics as well as tracking various cellular events.<sup>11</sup>

GFP contains a *p*-hydroxybenzylidene-imidazolidinone chromophore, which is generated by cyclization and oxidation of Ser-Tyr-Gly sequence at positions 65–67 (Fig. 2b). Since this chromophore is formed from the primary structure of the protein, GFP does not require the use of additional cofactors or substrates prior to *in vivo* imaging. However, wild-type GFP has some significant drawbacks that include a low fluorescent intensity and a low rate of formation of the chromophore after protein biosynthesis. To overcome these limitations, EGFP (enhanced GFP), which has more than thirty times brighter fluorescence than wild-type GFP, was developed by chromophore mutation of wild-type GFP (Fig. 2c). Later, a more diverse array of GFP variants with



**Juyoung Yoon**

investigations of fluorescent chemosensors, molecular recognition and organo EL materials.

Juyoung Yoon was born in Pusan, Korea in 1964. He received his PhD (1994) from Ohio State University. After completing postdoctoral research at UCLA and at Scripps Research Institute, he joined the faculty at Silla University in 1998. In 2002, he moved to Ewha Womans University, where he is currently a Professor of the Department of Chemistry and Nano Science and the Department of Bioinspired Science. His research interests include



**Injae Shin**

Assistant Professor of Chemistry at the Yonsei University in 1998 where he became Associate Professor in 2001 and Professor in 2006. His research interests include functional studies of glycans using chemical tools and the development of small molecules that affect biological processes.

Injae Shin was born in Daegu, South Korea, in 1962. He received his BS degree in Chemistry in 1985 and MS degree in 1987 from Seoul National University. His PhD studies were carried out at the University of Minnesota under the guidance of Professor Hung-wen Liu (1991–1995). He then moved to the University of California-Berkeley where he worked with Professor Peter Schultz as a postdoctoral fellow (1995–1998). He started his independent career as

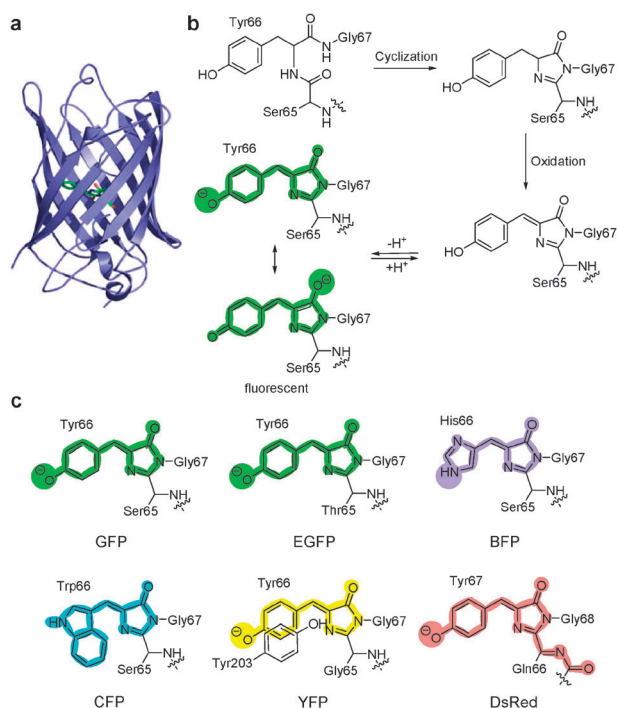


**Fig. 2** Fluorescent proteins. (a) X-Ray structure of GFP and (b) a biosynthetic pathway for the chromophore of GFP. The deprotonated chromophore displays green fluorescence. (c) Chemical structures of chromophores of various fluorescent proteins. Chromophores are highlighted based on the emission color.

**Table 1** Fluorescent properties of fluorescent proteins

Fluorescent protein	Ex <sub>max</sub> /nm	Em <sub>max</sub> /nm	Extinction coefficient/M <sup>-1</sup> cm <sup>-1</sup>	Quantum yield ( $\Phi$ )
GFP	395/475	509	21 000	0.77
EGFP	484	507	56 000	0.60
BFP	383	445	29 000	0.31
CFP	439	476	32 500	0.40
YFP	514	527	83 400	0.61
DsRed	558	583	75 000	0.79
DsRed-Monomer	556	586	35 000	0.10
HcRed	588	618	20 000	0.05
Dendra2	490 <sup>a</sup> (green)	507	45 000	0.50
	553 <sup>b</sup> (red)	573	35 000	0.55
asFP595	572	595	56 200	<0.001
Midori-Ishi Cyan	472	495	27 300	0.90
Kusabari Orange	548	559	51 600	0.60

<sup>a</sup> Before activation. <sup>b</sup> After activation.

blue (blue fluorescent protein, BFP), cyan (cyan fluorescent protein, CFP) and yellowish green emissions (yellow fluorescent protein, YFP) were developed through extensive mutagenesis investigations (Fig. 2c and Table 1).

In general, longer wavelength excitation of fluorescent proteins minimizes both phototoxicity (less cell damage by light) and background autofluorescence of cells and tissues, and it enables deeper probing of biological samples. Therefore, fluorescent proteins with red fluorescence emission have been prepared from species other than jellyfish. One of the proteins is tetrameric DsRed from the anemone *Discosoma* sp. that has emission maxima at 583 nm. Since wild-type DsRed has

serious drawbacks associated with its strong tendency to oligomerize and the slow maturation of its fluorescence signal, DsRed variants have been developed for imaging applications. One of the analogs is DsRed-Monomer that, in comparison with wild-type tetrameric DsRed, has a reduced tendency to form aggregates in fusion constructs. Another red fluorescent protein that is potentially more suitable for *in vivo* imaging is HcRed. This protein, produced by site-directed and random mutagenesis of a nonfluorescent chromoprotein from the anemone *Heteractis crista*, exhibits bright emission at 618 nm.<sup>12</sup> Although GFP variants and red fluorescent proteins have different chromophores and fluorescent properties (Table 1), they have similar three dimensional structures comprised of eleven  $\beta$ -strands that comprise a  $\beta$ -barrel with an  $\alpha$ -helix running through the center, and the chromophore that resides in the middle of the  $\beta$ -barrel (Fig. 2a).

Photoactivatable fluorescent proteins, whose fluorescence states can be regulated by irradiation with relatively intense light of appropriate wavelengths, have gained increasing popularity as tools for visualization of intracellular dynamics and high-resolution protein localization.<sup>13</sup> An example is found in Dendra2 from the octocoral *Dendronephthya* sp. which undergoes irreversible green-to-red photoswitching. This protein contains a chromophore that can exist in either a neutral (nonfluorescent) or an anionic (green fluorescent) state (Fig. 3a).<sup>14</sup> Upon irradiation at *ca.* 400 nm, the non-fluorescent neutral chromophore of the protein is efficiently converted to the red fluorescent state. On the other hand, excitation of Dendra2 by using intense blue light at *ca.* 490 nm results in a less efficient green-to-red photoconversion. It is known that Dendra2 undergoes photoswitching through a pathway involving cleavage of the protein backbone in the region of the chromophore.

Fluorescent proteins exhibiting reversible photoconversion between nonfluorescent and fluorescent states also have been developed. One example is found in the protein asFP595 from the anemone *Anemonia sulcata*, often referred to as a “kindling fluorescent protein”, that displays very weak fluorescence ( $\Phi_{\text{fluor}} < 0.001$ ).<sup>15</sup> However, upon irradiation with green light (*ca.* 570 nm) the chromophore isomerizes from a nonfluorescent *trans* to a red fluorescent *cis* state (Fig. 3b and c). Moreover, the fluorescent chromophore (*cis*) can be reconverted to the nonfluorescent analog (*trans*) by blue light irradiation at *ca.* 450 nm.

One of important applications of fluorescent proteins is in the exploration of spatio-temporal patterns of biological events using the nondestructive spectroscopic method referred to as fluorescence resonance energy transfer (FRET). FRET, which relies on the distance-dependent transfer of energy from a fluorescent donor to a fluorescent acceptor, can be employed to monitor the proximity of a donor and an acceptor in living cells and organisms. Consequently, this technique can be applied to probe a variety of biological phenomena, including biomolecular interactions, enzymatic reactions and structural changes (Fig. 4). Most FRET studies carried out thus far using fluorescent proteins have employed CFP and YFP as the respective FRET donor and acceptor (Fig. 4a). However, the use of this pair has some drawbacks such as a relatively high sensitivity to pH and bleeding between channels. A more

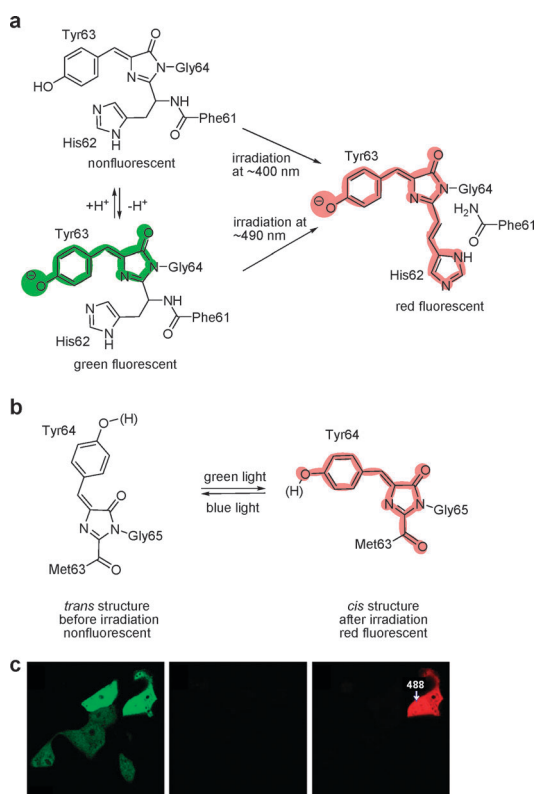


**Fig. 3** Photoswitching of Dendra2 and asFP595. (a) Irreversible photoswitching of Dendra2. (b) Reversible photoswitching of asFP595. (c) Photoswitching of Dendra2 in cells. Left and middle panels: fluorescent images of cells before photoconversion. (left) The image was taken after weak irradiation at 488 nm for detection at 500–540 nm (green channel). (middle) The image was taken after modest irradiation at 543 nm for detection at 560–680 nm (red channel). Right panel: fluorescent image of cells after photoconversion of one cell by intense 488 nm irradiation (excitation at 543 nm, detection at 560–680 nm, red channel). (Reprinted from ref. 14 with permission.)

recently developed protein pair, composed of Midori-Ishi Cyan as a donor and Kusabari Orange as an acceptor, has been found to exhibit brighter fluorescence and better spectral separation between the donor and acceptor fluorescence signals than is observed with the CFP–YFP pair.<sup>16</sup> In addition, this pair shows a substantially low pH dependence of the donor fluorescence quantum yield and the acceptor absorption wavelength. As a result, the Midori-Ishi Cyan–Kusabari Orange pair is highly suitable for quantitative FRET imaging.

## 2.2 Applications of fluorescent proteins to zebrafish imaging

Proteins are perhaps the most amenable biomolecules for *in vivo* imaging since they can be readily manipulated to produce chimeras fused to fluorescent proteins. The localizations and dynamics of proteins in cells and organisms can be visualized by using proteins fused to fluorescent proteins.<sup>17–19</sup> In addition, the fusion proteins can also enable spatio-temporal tracing of the fate of cells in developing embryos. Moreover, combination of fluorescent proteins with different emission wavelengths leads to multicolor imaging of live cells and animals in differential gene expression and protein localization studies.<sup>20</sup>

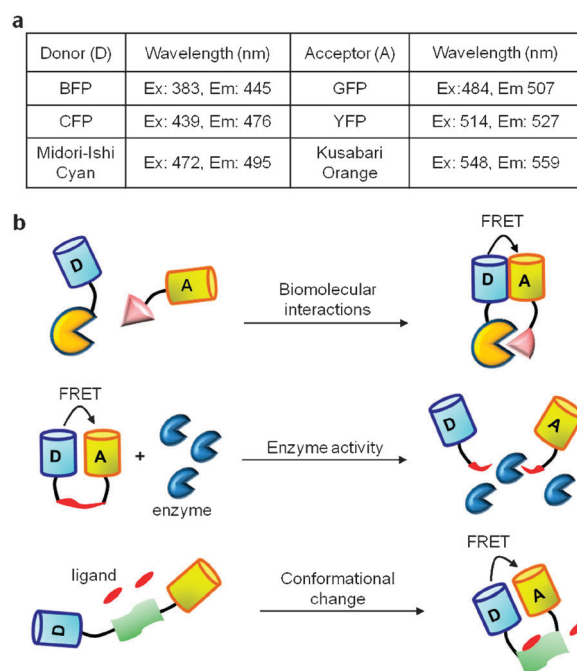


**Fig. 4** Applications of FRET for bioscience. (a) Fluorescent protein pairs for FRET. (b) FRET can be used to study biomolecular interactions and enzyme activity as well as to probe conformational changes induced by ligand binding.

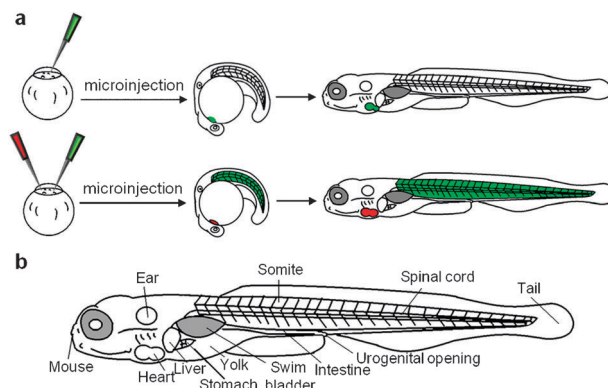


**Fig. 5** Transgenic zebrafish for *in vivo* imaging. (a) Single or double fluorescent protein genes fused to tissue-specific genes are injected into embryos to visualize specific tissues. (b) Drawing of a five day old zebrafish. Organs can be observed by microscopy due to transparency of embryos.

Owing to their transparency, external fertilization and easy genetic manipulation, zebrafish embryos are particularly applicable to *in vivo* imaging using genetically encoded fluorescent proteins. By utilizing the transgenic technology, a foreign fluorescent protein gene either by itself or as a part of a fusion protein can be introduced into zebrafish embryos (Fig. 5).<sup>21,22</sup> A variety of transgenic zebrafish expressing fluorescent proteins in specific tissues were produced to track cell fate in developing embryos. For example, heart development was visualized in real-time by using transgenic zebrafish expressing EGFP specifically in heart. In addition, this transgenic zebrafish was used to study abnormal heart developmental processes induced by synthetic small molecules.<sup>23</sup>

Transgenic zebrafish carrying fluorescent proteins was also used to visualize apoptotic cells during development at a high spatial and temporal resolution. In this effort, zebrafish was constructed to contain a YFP fused to a secretion signal peptide and Annexin V that binds to phosphatidyl serine exposed on the outer leaflet of the plasma membrane during apoptosis. Using this transgenic organism, patterns of apoptosis in living zebrafish embryos were characterized.<sup>24</sup> In addition, imaging of neuronal cell death was performed by using fluorescently labeled TAU transgenic zebrafish.<sup>25</sup> Furthermore, transgenic zebrafish expressing two different fluorescent proteins was employed for dual-channel fluorescence based two-color imaging of the differential development of tissues and cell-cycle progression in the developing zebrafish embryos.<sup>26,27</sup>

The two-photon effect consists of electronic excitation of a chromophore by simultaneous absorption of two near-infrared photons within a femtosecond time scale.<sup>28</sup> Since two-photon excitation enables the use of longer wavelength light, events that take place deeper in tissues can be visualized without causing significant cell damage. This approach was exploited to observe gene expression deep inside developing embryos.<sup>29</sup> For this purpose, a heart-specific gene fused to HcRed with an emission peak at 618 nm was injected into zebrafish embryos.<sup>30</sup> Using the two-photon fluorescence microscopy method and an excitation laser with a wavelength of 1230 nm, two-photon fluorescence images of the developing heart deep inside live zebrafish were successfully recorded.

In addition to using fluorescent proteins to image biological events, cleverly designed fluorescent proteins were applied to specifically monitor biologically relevant ions or chemical contaminants in zebrafish. Free  $\text{Ca}^{2+}$  in the cytosol and organelles play important roles in cellular signaling. Thus, the detection of intracellular calcium ions is crucial for understanding their biological roles. For measurements of dynamic and quantitative  $\text{Ca}^{2+}$  concentrations, cameleon, in which CFP and YFP are linked by calmodulin and a M13 calmodulin-binding domain, was constructed (Fig. 6).<sup>31,32</sup>  $\text{Ca}^{2+}$  in cells binds to calmodulin and causes an interaction with M13 that induces a conformational change of the protein. This change enhances the efficiency of FRET from CFP to YFP. As a result, an increase in calcium concentrations can be

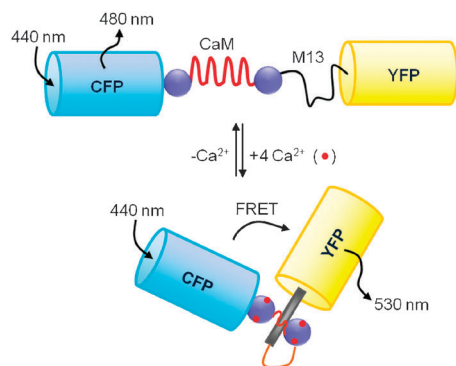


**Fig. 6** Schematic structure of cameleon to detect calcium ions. Upon increase in  $\text{Ca}^{2+}$  concentration, calmodulin (CaM) binds calcium ions and interacts with M13, which induces a conformational change of the protein. This change leads to increase in the efficiency of FRET from CFP to YFP.

determined by measuring the increase in the YFP/CFP fluorescence intensity ratio. Using the transgenic zebrafish expressing a neuron-specific cameleon, calcium concentration changes in neurons in active zebrafish were successfully monitored.<sup>33</sup>

Reactive oxygen species, including hydrogen peroxide ( $\text{H}_2\text{O}_2$ ), are involved in important biological processes such as cellular signaling and pathologic events. To understand the biological roles of hydrogen peroxide, researchers have constructed a  $\text{H}_2\text{O}_2$ -specific, genetically encoded biosensor called 'HyPer' by fusing YFP to the regulatory domain of OxyR that modulates transcription in response to  $\text{H}_2\text{O}_2$ .<sup>34</sup> A regulatory domain of OxyR in HyPer senses  $\text{H}_2\text{O}_2$  through the oxidation of a cysteine residue. This process results in a dramatic conformational change and concomitantly leads to an increase in the fluorescence of YFP at 516 nm. HyPer exhibits a fluorescent signal in response to submicromolar concentrations of  $\text{H}_2\text{O}_2$  but it does not respond to other reactive oxygen species. This HyPer sensor has been utilized to probe the role of  $\text{H}_2\text{O}_2$  during the early events associated with wound responses in zebrafish.<sup>35</sup> The results show that hydrogen peroxide is generated by a protein called dual oxidase three minutes following a local cut induced injury of zebrafish. It is proposed that a concentration gradient of the generated hydrogen peroxide guides leukocytes to the wound in order to defend against pathogens.

Mercury is one of the most prevalent toxic metals in the environment. This metal ion easily passes through biological membranes and causes damage to the central nervous and the endocrine system. With the purpose of developing a sensitive method to monitor low levels of mercury ions, the transgenic zebrafish that produces a luciferase–GFP fusion protein under conditions of the oxidative stress was constructed.<sup>36</sup> In this system, the GFP component enables visual detection of mercury while the activity of the luciferase component allows quantitative measurement of gene expression in embryo extracts. Upon exposure to mercury ions, an increase in fluorescence intensity occurs in various tissues in developing zebrafish through the intracellular oxidative stress response elicited by mercury. The studies using the transgenic zebrafish expressing fluorescent proteins clearly reveal that zebrafish is a valuable tool for the spatio-temporal detection and analysis of many biological processes.

### 3. Zebrafish imaging using synthetic fluorescent probes

#### 3.1 Visualization of biomolecules in zebrafish

As discussed above, zebrafish serves as a very useful vertebrate model for molecular imaging owing to the fact that the location and expression patterns of proteins can be visualized. In addition, small molecules and ion species can be also monitored in zebrafish by using the cleverly designed fluorescent proteins. However, fluorescent proteins used for live animal imaging can sometimes interfere with the function of proteins of interest or suffer from drawbacks such as the lack of selectivity. Alternatively, owing to their easy manipulation and relatively high sensitivities synthetic fluorescent probes

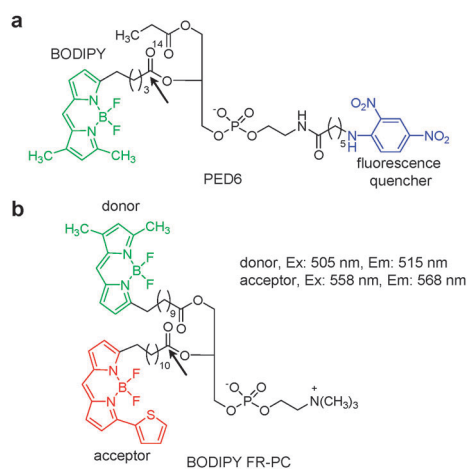


**Fig. 7** Fluorescent dyes to monitor PLA<sub>2</sub> activity in zebrafish. (a) PED6 possesses BODIPY as a fluorophore and dinitrophenyl group as a quencher. (b) BODIPY FR-PC contains a donor and an acceptor for FRET.

have been widely used for *in vivo* visualization of (bio)molecules and biologically relevant species.

For example, enzyme activities in living animals have been monitored using synthetic dyes for the purpose of investigating their functional profiling rather than expression levels. Phospholipase A<sub>2</sub> (PLA<sub>2</sub>) catalyzes the cleavage of the *sn*-2 fatty acyl bond of glycerophospholipids to release lysophospholipid and free fatty acid, both of which are potential precursors to lipid signaling molecules. Synthetic fluorescent phospholipid reporters, such as fluorescently quenched (PED6) and tagged phospholipids (BODIPY FR-PC) that are substrates for PLA<sub>2</sub>, were prepared for visualization of PLA<sub>2</sub> activity in zebrafish (Fig. 7).<sup>37</sup> Hydrolysis of PED6 by PLA<sub>2</sub> results in restoration of fluorescence of BODIPY, thus enabling imaging of PLA<sub>2</sub> activity in zebrafish embryos (Fig. 7a). BODIPY FR-PC, possessing a donor and an acceptor for FRET, was employed to determine the site of PLA<sub>2</sub> activity more precisely (Fig. 7b). Prior to cleavage of this probe by PLA<sub>2</sub>, excitation of a donor at 505 nm produces an orange emission at 568 nm from an acceptor *via* the FRET effect. However, when an acceptor is removed from BODIPY FR-PC by PLA<sub>2</sub>, a green emission at 515 nm is observed. Therefore, distinct fluorescent signals are produced before and after cleavage of the probe by PLA<sub>2</sub>. The observation that zebrafish incubated with PED6 and BODIPY FR-PC exhibits strong fluorescence in the gall bladder associated with PLA<sub>2</sub> activity demonstrates that fluorescent phospholipid reporters can provide a sensitive readout of lipid metabolism in live animals.

Another application of synthetic fluorescent probes for assessing enzyme activity is found in the detection of oxidative catalysis by cytochrome P450. The cytochrome P450 superfamily is composed of a group of proteins involved in the metabolism of a wide variety of xenobiotics, including drugs and toxic chemicals as well as endogenous molecules such as lipids and steroidal hormones. The most common reaction catalyzed by this enzyme family is a monooxygenase reaction, *e.g.*, insertion of one atom of molecular oxygen into an organic

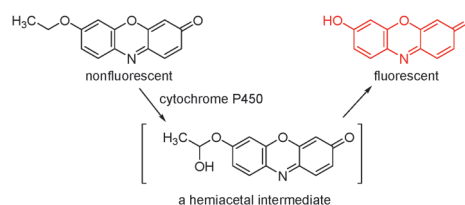


**Fig. 8** Ethylresorufin to sense cytochrome P450 activity. Non-fluorescent ethylresorufin is converted to hemiacetal by cytochrome P450 followed by spontaneous decomposition of hemiacetal to produce fluorescent resorufin.

substrate while the other oxygen atom is reduced to water. Since fish overexpresses cytochrome P450 when exposed to aquatic contaminants such as dioxins, fish cytochrome P450 is a widely accepted environmental biomarker. For an *in vivo* assay of cytochrome P450 activity, zebrafish exposed to dioxins was incubated with nonfluorescent ethylresorufin which serves as a substrate for this enzyme.<sup>38</sup> In contrast to untreated zebrafish that exhibits very low fluorescence due to its very low intrinsic cytochrome P450 activity, dioxin-treated zebrafish displays intense fluorescence associated with resorufin that is generated by oxidative cleavage of ethylresorufin promoted by the overexpressed enzyme (Fig. 8).

Cell-surface glycans play key roles in a variety of physiological and pathological processes through their interactions with proteins.<sup>39</sup> Accordingly, they are important targets for *in vivo* imaging. Glycans are biosynthesized in a template-independent manner *via* stepwise processes promoted by glycosyltransferases and glycosidases. Because of this feature, glycan imaging is incompatible with systems based on genetically encodable fluorescent protein reporters and thus is challenging. A two-step approach was recently developed to visualize glycans *in vivo*.<sup>40</sup> This method involves the metabolic incorporation of a non-native sugar, conjugated with a bioorthogonal functional group, into a target glycan in live animals. This step is followed by chemoselective labeling of the bioorthogonal functional group with a fluorescent probe. The azide moiety is a suitable bioorthogonal group for this purpose owing to its small size, stability in biological systems, and selective reactivity with specific functional groups such as phosphines or activated alkynes. Peracetylated *N*-azidoacetyl-galactosamine (Ac<sub>4</sub>GalNAz), a cell and organism-permeable functionalized monosaccharide, was chosen as a metabolic substrate since it is known to be incorporated into mucin-type *O*-linked glycoproteins in mammalian cells and mice (Fig. 9a). For visualization of glycans in a live animal, zebrafish embryos were initially incubated with Ac<sub>4</sub>GalNAz to metabolically label cell-surface glycans with azides (Fig. 9b). Subsequently, the embryos were treated with a difluorinated cyclooctane-conjugated fluorophore that selectively reacts with azide *via* a Cu(I)-free strain-promoted cycloaddition. This procedure enabled *in vivo* visualization of glycans at subcellular resolution during zebrafish development. In addition to single color imaging, multi-color visualization of glycans was also performed. For this purpose, zebrafish embryos, which were incubated sequentially with Ac<sub>4</sub>GalNAz and the first fluorophore, were treated with tris-(2-carboxyethyl)phosphine (TCEP) to remove unreacted azide groups (Fig. 9b). The TCEP-treated embryos

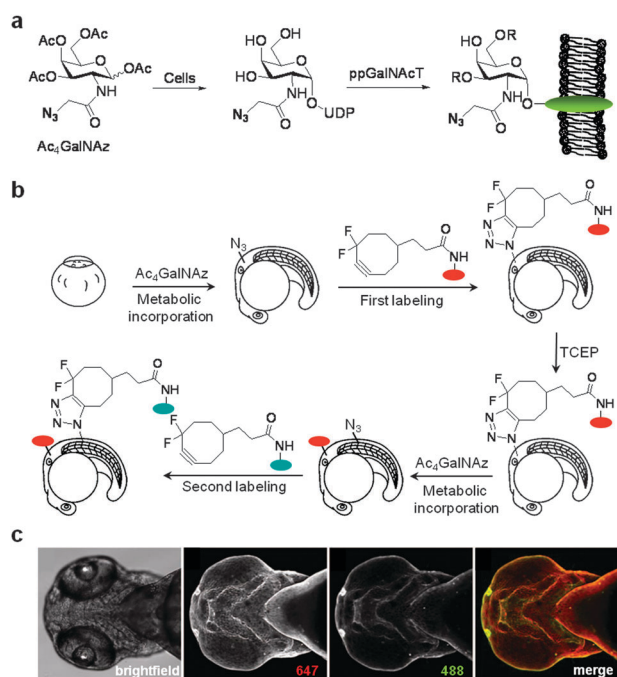


**Fig. 9** Detection of glycans in zebrafish. (a) Metabolic incorporation of cell-surface glycans with GalNAz (ppGalNAcT; polypeptide *N*-acetyl- $\alpha$ -galactosaminyltransferase). (b) A multicolor labeling strategy of zebrafish using different fluorescent dyes. (c) Two-color labeling of *O*-glycans in live zebrafish (red: the first labeling of azides with difluorinated cyclooctane-conjugated Alexa Fluor 647, green: the second labeling of azide with difluorinated cyclooctane-conjugated Alexa Fluor 488). (Reprinted from ref. 40 with permission.)

were then sequentially treated with Ac<sub>4</sub>GalNAz and the second fluorophore (Fig. 9c). The multi-color imaging technique led to resolution of temporally distinct populations of glycans in zebrafish that would have been undetectable using conventional molecular imaging approaches. As a consequence, the two-step imaging procedure is a valuable tool for viewing glycans in developing zebrafish and it broadens the array of tools that are available for probing the dynamic glycome.

Intracellular thiols, such as cysteine, homocysteine and glutathione, play a variety of crucial roles in physiological systems. The levels of these substances can change dramatically in response to oxidative stress associated with toxic insults, bacterial infection and disease. Also, abnormal intracellular thiols are the cause of various health problems. Therefore, the detection of thiol-containing molecules in biological samples is of great importance. The fluorescein-based probe **1** has been developed for the highly selective and sensitive detection of biological thiols in zebrafish (Fig. 10).<sup>41</sup> If thiol species attacks the  $\alpha,\beta$ -unsaturated ketone moiety in **1**, then the spiro group undergoes ring opening to produce a product that possesses enhanced fluorescence. Importantly, a strong fluorescence was exhibited by zebrafish that was incubated with **1**. However, when zebrafish were pretreated with *N*-methylmaleimide, which is a trapping reagent of thiols, a remarkable decrease in fluorescence intensity was observed, indicating that thiols were selectively monitored by **1**.

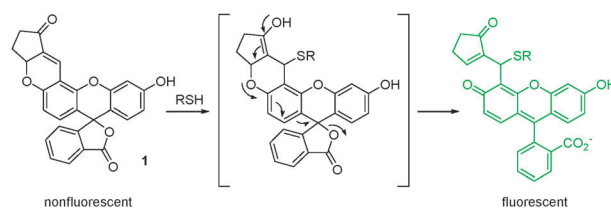


**Fig. 10** A thiol-selective fluorescent chemosensor used for *in vivo* imaging.

Tissue specific fluorescent dyes are valuable substances for investigating complex physiological and pathological processes. Recently, zebrafish embryos were shown to be useful for the identification of synthetic fluorescent dyes from a fluorescent dye library that selectively sense neurons.<sup>42</sup> Fluorescence microscopy screening provided a few dyes that selectively stain neurons. Although their binding sites are not known, the dyes could be used as indicators to study neuron-related biological processes and to monitor environmental toxic materials that destroy neurons.

### 3.2 Monitoring of biologically relevant species in zebrafish

In addition to its use for visualization of biomolecules with synthetic organic dyes, zebrafish has been employed as a vertebrate model for *in vivo* monitoring of biologically relevant species using fluorescent chemosensors. As mentioned above, inorganic and organic mercury compounds are environmentally prevalent, toxic species. As a result, monitoring of these substances is of great importance to human health. To date, various fluorescent chemosensors have been developed for *in vitro* and *in vivo* detection of mercury species. Among these sensors, the rhodamine-based chemodosimeter **2** has received great attention.<sup>9,43</sup> This sensor responds to mercury ions in a stoichiometric, rapid and irreversible manner to generate a product that is strongly fluorescent (Fig. 11a). When zebrafish embryos were exposed to mercury ions and **2**, strong fluorescence intensities were observed inside zebrafish, indicating that the probe is organism-permeable (Fig. 11e). In addition, real-time mercury-ion uptake in zebrafish was monitored by using **2**. The results of these studies showed that mercury-ion uptake by zebrafish reached a maximum value within 20–30 min. Following a similar mechanism, **2** also reacts irreversibly with methylmercury in zebrafish in a highly sensitive fashion.<sup>44</sup> These studies served as the foundation for monitoring of biologically relevant species in live zebrafish.

Recently, the selenolactone-based chemosensor **3** was developed for detection of inorganic and organic mercury species.<sup>45</sup> This probe senses mercury species with a high selectivity and sensitivity by way of fluorescence response induced by the mercury ion-promoted deselenation reaction shown in Fig. 11b. The value of this system was successfully demonstrated by its use in detecting mercury species in cells and zebrafish. Another mercury-selective fluorescent sensor, vinyl ether fluorescein **4**, has been prepared and demonstrated to undergo a fluorescence enhancement *via* a mercury ion-accelerated hydrolysis of the vinyl ether moiety (Fig. 11c).<sup>46</sup> Studies aimed at evaluating the capability of monitoring mercury species in live organisms revealed that probe **4** effectively senses mercury species in zebrafish.

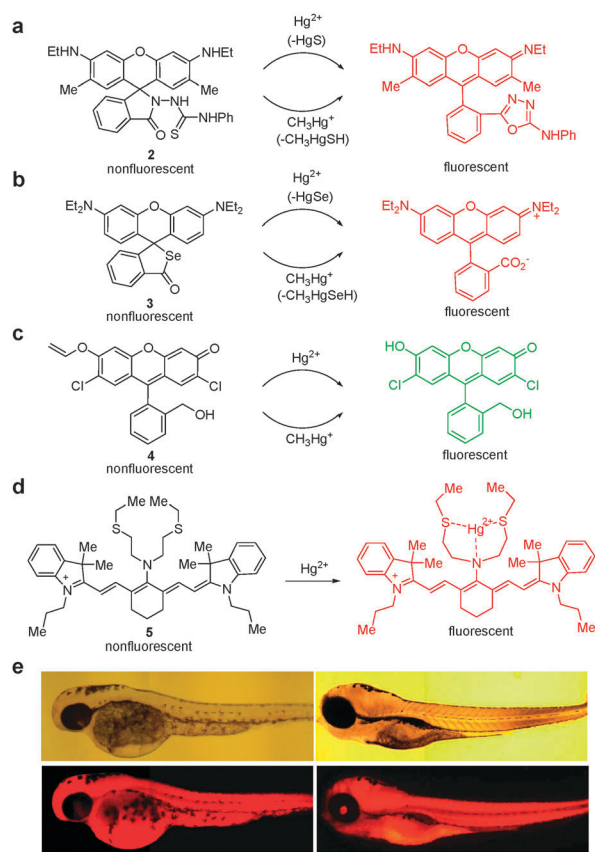


**Fig. 11** (a–d) Mercury-selective fluorescent chemosensors used for *in vivo* imaging. (e) Images of a 3 day-old (left) and a 5 day-old zebrafish (right) treated with both **2** and mercury ions (top, microscopic image; bottom, fluorescence microscopic image).

A near-infrared fluorescent probe **5** was also devised for detecting mercuric ions in biological systems (Fig. 11d).<sup>47</sup> This probe, which stoichiometrically, rapidly and reversibly produces a fluorescent response, coordinates with mercury ions to generate a complex in which a photoinduced electron transfer quenching of the excited state of the probe is blocked. *In vivo* imaging experiments showed that a strong fluorescence pattern is generated in zebrafish exposed to both mercury ions and **5**.

The mercury-selective probes described above hold great potential in studies probing the accumulation and toxicity of mercury species in living organisms. In addition to fluorescent chemosensor-based methods to detect mercury species in zebrafish, an approach using synchrotron X-ray fluorescence imaging has been developed.<sup>48</sup> This methodology was found to be suitable for monitoring the accumulation of mercury species in zebrafish and may also be used as an alternative tool for investigating molecular toxicology of other heavy metals.

Zinc is an essential cofactor in many biological processes such as brain function and pathology, gene transcription and mammalian reproduction. Biological imaging of  $\text{Zn}^{2+}$  ions can provide direct information on the spatio-temporal distributions of this ion in living systems. For this purpose, a NBD (nitrobenzoxadiazolyl)-based  $\text{Zn}(\text{II})$ -selective sensor **6** was recently developed (Fig. 12a).<sup>49</sup> This probe exhibits

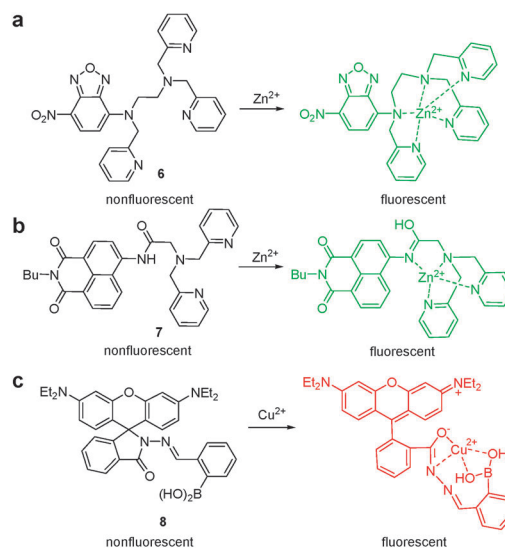


**Fig. 12** Fluorescent chemosensors used to monitor zinc/copper ions in zebrafish.

selective  $\text{Zn}^{2+}$ -amplified fluorescence through a mechanism involving coordination of nitrogens in the probe with  $\text{Zn}^{2+}$ . Using this sensor, intact zinc ions were clearly monitored at two zygomorphic areas around the ventricle in zebrafish. Furthermore, high concentrations of  $\text{Zn}^{2+}$  in the developing neuromasts of zebrafish were also visualized by confocal fluorescence imaging. More recently, the naphthalimide-based fluorescent probe **7**, which contains an amide-DPA receptor, was developed for ratiometric  $\text{Zn}^{2+}$  sensing (Fig. 12b).<sup>50</sup> Probe **7** showed excellent selectivity for  $\text{Zn}^{2+}$  over other metal ions along with an enhanced and red-shifted fluorescence emission. When zebrafish embryos at different stages of development were incubated with probe **7**, intact zinc ions were clearly detected by using fluorescence microscopy.

Copper ions play a critical role as a catalytic cofactor for a variety of metalloenzymes, including superoxide dismutase, cytochrome *c* oxidase and tyrosinase. Owing to the biological significance of copper ions, the copper-selective sensor **8**, based on a boronic acid-conjugated rhodamine platform, was developed (Fig. 12c).<sup>51</sup> The binding of  $\text{Cu}^{2+}$  to **8** induces opening of the spirolactam ring to produce a fluorescent rhodamine derivative. *In vivo* imaging experiments using zebrafish showed that copper ions can be fluorescently detected by utilizing **8**.

Nitric oxide (NO) is involved in many physiological functions such as vasodilatation, bronchodilatation, neurotransmission and immune response. To investigate the detailed nature of its biological functions, the diaminofluorescein-based probe **9** was prepared and used as a fluorescent NO sensor (Fig. 13a).<sup>52</sup> When this probe enters cells or organisms, its acetyl groups are removed by the action of intracellular esterases. Subsequently, the resulting product traps intracellular NO *via* a nitrosation and dehydration sequence to generate a highly fluorescent triazolofluorescein derivative. NO production in live zebrafish was successfully monitored using this probe. In addition, the specificity of the fluorescence response of **9** to NO was confirmed by observing both a



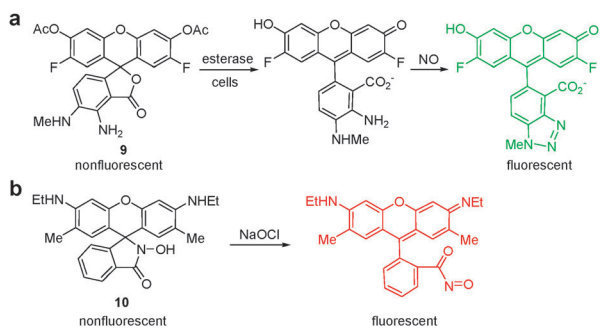


**Fig. 13** Fluorescent chemosensors to detect reactive oxygen species *in vivo*. (a) Nitric oxide chemosensor and (b) hypochlorite chemosensor.

decrease in fluorescence intensity in animals exposed to a NO scavenger or a NO synthase inhibitor and an increase in the presence of a NO donor.

Hypochlorite ion ( $\text{ClO}^-$ ), one of the reactive oxygen species (ROS), plays various roles in biological systems. Owing to its highly reactive and diffusible nature, uncontrolled production of hypochlorite derived from phagocytes is involved in a variety of human diseases such as neurodegenerative, cardiovascular and inflammatory diseases. The detailed understanding of the role of hypochlorite in biology and medicine has been hampered by the lack of a selective and sensitive detection method. Recently, the selective and sensitive fluorescent chemosensor **10** was devised for the detection of hypochlorite (Fig. 13b).<sup>53</sup> Whereas zebrafish treated only with probe **10** was found to exhibit no fluorescence, strong red fluorescence was observed in zebrafish exposed to both NaOCl and **10**. It was suggested that fluorescence response of **10** to hyperchlorite ions takes place through generation of a highly fluorescent acyl nitroso product *via* oxidation of a hydroxamic acid moiety in **10** by hyperchlorite ions.

Palladium is an important metal used in dental and medicinal devices and catalytic converters. However, complexes of this metal adversely affect human health since palladium ions can interact with biomolecules in a manner that perturbs many biological processes. Therefore, investigations aimed at the discovery of new methodology for selective and sensitive detection of palladium ions have received great attention. In one effort in this area, the fluorescein-based probe **11** was developed for *in vivo* monitoring of palladium species (Fig. 14).<sup>54</sup> It was suggested that **11** becomes fluorescent as a result of a palladium-promoted depropargylation reaction. When zebrafish embryos were treated with palladium and **11**, strong green fluorescence was observed. The *in vivo* imaging studies described above demonstrate that zebrafish is a useful vertebrate model for visualization of biologically relevant species as part of toxicity and bioactivity investigations.

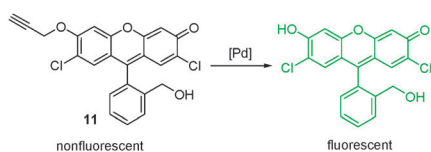


**Fig. 14** palladium-selective fluorescent chemosensor used for *in vivo* imaging.

#### 4. Zebrafish imaging using quantum dots

Fluorescent proteins and synthetic fluorescent dyes are very useful for imaging analytes in live cells and organisms. However, these types of probes have some drawbacks including relatively low photostability. Quantum dots (QDs), fluorescent semiconductor nanocrystals, offer an attractive alternative for *in vivo* imaging as a result of unique properties that are unmatched by fluorescent proteins and fluorescent organic dyes.<sup>8,55</sup> QDs emit greater than one hundred times more strongly than synthetic dyes. In addition, they can be fine-tuned to fluoresce in almost any color by controlling their size and have a broad excitation band and a relatively narrow emission band. These properties of QDs allow an easy separation of emission signals and the simultaneous detection of multiple colors by irradiation at a single excitation wavelength. Importantly, QDs are photostable and, thus, they do not lose fluorescence when exposed to light over long periods. Accordingly, they can be directly monitored in living cells and organisms for an extended period of time. Overall, QDs allow long-term and multiple color imaging of cellular and molecular events.

An initial application of the QD methodology to live organism imaging was aimed at the visualization of *Xenopus* embryos using ZnS-overcoated CdSe (ZnS/CdSe) QDs encapsulated in biocompatible phospholipid micelles.<sup>56</sup> When injected into *Xenopus* embryos, the QD-micelles showed very low toxicity, thus, enabling the cell lineage in embryos to be successfully traced by fluorescence visualization. In addition, the QD-micelles were stable to degradation and resistant to photobleaching in embryos and, as a result, fluorescence remained detectable during the course of the experiments.

After this work, zebrafish embryos were fluorescently imaged using streptavidin-conjugated ZnS/CdSe QDs to understand cellular behavior during their developmental processes.<sup>57,58</sup> Zebrafish embryos injected with QDs into their heart ventricles showed strong fluorescence in the vascular system of zebrafish, ranging from early differentiation to late embryonic stages. Since QDs employed for this study were not toxic to embryos, imaging experiments could be repeatedly performed to observe newly formed vessels. In addition, using GFP or RFP-transgenic zebrafish embryos injected with QDs, spatial patterns of the vascular and the nervous system of zebrafish were also visualized (Fig. 15).

The above studies demonstrate that QDs have great potential for visualizing biological processes in live animals. However, QD approach needs to be improved in order to

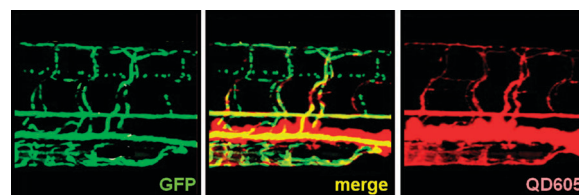


**Fig. 15** Two-color images of the trunk of zebrafish embryos using GFP and QDs. GFP is expressed in erythrocytes and neurons of transgenic zebrafish. The vasculature in zebrafish exhibits red fluorescence by QDs.<sup>57</sup>

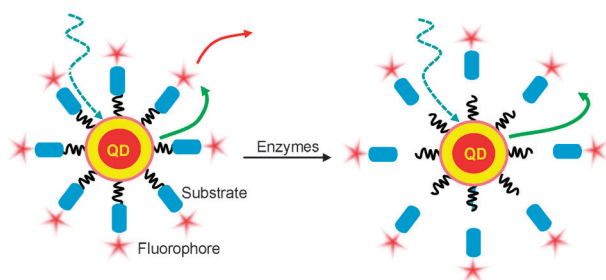


**Fig. 16** FRET-based QD sensors. The QD sensors are composed of QDs and coated substrates that are linked by dyes.

broaden applications for live animal imaging. For example, QDs are not organism-permeable and thus they are generally injected into embryos. To overcome this limitation, QDs can be modified with suitable materials that enhance their permeability into live embryos. More importantly, QDs-based biosensors that respond selectively to analytes such as biomolecules and biologically relevant species should be developed to monitor specific analytes in live organisms. Recently, FRET-based QD sensors were developed for *in vitro* studies.<sup>59</sup> The QD sensors are composed of QDs and coated substrates that are linked by dyes. In these sensors, the fluorescence of QDs is quenched *via* FRET by other dyes linked to QDs. Importantly, their fluorescence is restored by release of the linked dyes promoted by analytes such as enzymes (Fig. 16). Ultimately, the availability of analyte-selective, organism-permeable QDs will broaden their use in animal imaging to probe many biological events.

## 5. Conclusions

Owing to its small size, optical transparency, external fertilization and easy manipulation, zebrafish is perhaps the most suitable vertebrate model animal for *in vivo* imaging using fluorescent probes. In this review, we have discussed the usefulness of zebrafish for visualization of the localization and dynamics of biomolecules, such as proteins, lipids and glycans, and for real-time monitoring of biologically relevant species. In addition, more complex biological processes such as embryonic protein movements, cellular interactions and subcellular dynamics within live zebrafish can be also probed using fluorescent probes.

However, a number of challenges remain regarding the development of fluorescent probes and their *in vivo* imaging applications. Many synthetic organic dyes are cell and organism-permeable and, thus, they can be introduced into zebrafish by simply adding the dyes to incubation media. In contrast, in order to introduce fluorescent proteins into live animals, genes either by themselves or as a part of fusion proteins need to be injected into animals. QDs, which are usually organism-impermeable, also need to be introduced into zebrafish by microinjection. To expand the usefulness of zebrafish for *in vivo* imaging, organism-permeable probes, in particular, QDs, should be developed thoroughly, which is a highly challenging task.

Another important challenge is to exploit more diverse ratiometric fluorescent probes, which are compatible with

zebrafish. These probes would enable quantification of dynamic changes in analytes within localized regions of live animals. In addition, targeted and activatable smart imaging sensors should be developed for selective visualization of analytes in zebrafish. Furthermore, more diverse near-infrared or two-photon fluorescent probes are required in order to visualize deep tissues or organs in animals with reduced damage of biosample and/or to maximize signal-to-noise ratios. On the other hand, fluorescent probes that selectively respond to diverse analytes, such as lipids, glycans, proteins and biologically relevant species, should be devised to expand the applications for *in vivo* imaging. Continuing efforts in this area hold great promise for visualization of a variety of analytes in zebrafish and suggest that a bright future exists for understanding complex biological processes in vertebrate organisms.

## Acknowledgements

This work was supported by grants from the National Creative Research Initiative Program, WCU (R32-2008-000-10217-0), National Research Foundation of Korea (NRF) (2010-0018895) and the Converging Research Center Program through the Ministry of Education, Science and Technology (2010K001202).

## References

- 1 D. W. Domaille, E. L. Que and C. J. Chang, *Nat. Chem. Biol.*, 2008, **4**, 168–175.
- 2 X. Chen, Y. Zhou, X. Peng and J. Yoon, *Chem. Soc. Rev.*, 2010, **39**, 2120–2135.
- 3 K. Kikuchi, *Chem. Soc. Rev.*, 2010, **39**, 2048–2053.
- 4 T. Samamoto, A. Ojida and I. Hamachi, *Chem. Commun.*, 2009, 141–152.
- 5 J. S. Kim and D. T. Quang, *Chem. Rev.*, 2007, **107**, 3780–3799.
- 6 Z. Xu, J. Yoon and D. R. Spring, *Chem. Soc. Rev.*, 2010, **39**, 1996–2006.
- 7 N. C. Shaner, P. A. Steinbach and R. Y. Tsien, *Nat. Methods*, 2005, **2**, 905–909.
- 8 I. L. Medintz, H. T. Uyeda, E. R. Goldman and H. Mattoussi, *Nat. Mater.*, 2005, **4**, 435–446.
- 9 S.-K. Ko, Y.-K. Yang, J. Tae and I. Shin, *J. Am. Chem. Soc.*, 2006, **128**, 14150–14155.
- 10 For detailed information, see homepage at Olympus Microscopy Resource Center Confocal Microscopy—The Fluorescent Protein Color Palette.htm.
- 11 J. Zhang, R. E. Campbell, A. Y. Ting and R. Y. Tsien, *Nat. Rev. Mol. Cell Biol.*, 2002, **3**, 906–918.
- 12 N. G. Gurskaya, A. F. Fradkova, A. Terskikh, M. V. Matz, Y. A. Labas, V. I. Martynov, Y. G. Yanushevich, K. A. Lukyanov and S. A. Lukyanov, *FEBS Lett.*, 2001, **507**, 16–20.
- 13 K. A. Lukyanov, D. M. Chudakov, S. Lukyanov and V. V. Verkhusha, *Nat. Rev. Mol. Cell Biol.*, 2005, **6**, 885–891.
- 14 D. M. Chudakov, S. Lukyanov and K. A. Lukyanov, *Nat. Protoc.*, 2007, **2**, 2024–2032.
- 15 M. Andresen, M. C. Wahl, A. C. Stiel, F. Gräter, L. V. Schäfer, S. Trowitzsch, G. Weber, C. Eggeling, H. Grubmüller, S. W. Hell and S. Jakobs, *Proc. Natl. Acad. Sci. U. S. A.*, 2005, **102**, 13070–13074.
- 16 S. Karasawa, T. Araki, T. Nagai, H. Mizuno and A. Miyawaki, *Biochem. J.*, 2004, **105**, 17789–17794.
- 17 S. Wang and T. Hazelrigg, *Nature*, 1994, **396**, 400–403.
- 18 R. Y. Tsien, *Annu. Rev. Biochem.*, 1998, **67**, 509–544.
- 19 M. Chalfie, Y. Tu, G. Euskirchen, W. W. Ward and D. C. Prasher, *Science*, 1994, **263**, 802–805.

- 20 A. F. Fradkov, Y. Chen, L. Ding, E. V. Barsova, M. V. Matz and S. A. Lukyanov, *FEBS Lett.*, 2000, **479**, 127–130.
- 21 E. Shafizadeh, H. Huang and S. Lin, *Methods Mol. Biol. (Totowa, N. J.)*, 2002, **183**, 225–223.
- 22 B. Ju, Y. Xu, J. He, J. Liao, T. Yan, C. L. Hew, T. J. Lam and Z. Gong, *Dev. Genet.*, 1999, **25**, 158–167.
- 23 S.-K. Ko, H. J. Jin, D.-W. Jung, X. Tian and I. Shin, *Angew. Chem., Int. Ed.*, 2009, **48**, 7809–7812.
- 24 T. J. van Ham, J. Mapes, D. Kokel and R. T. Peterson, *FASEB J.*, 2010, **24**, 4336–4342.
- 25 D. Paquet, R. Bhat, A. Sydow, E.-M. Mandelkow, S. Berg, S. Hellberg, J. Fälting, M. Distel, R. W. Köster, B. Schmid and C. Haass, *J. Clin. Invest.*, 2009, **119**, 1382–1395.
- 26 M. Sugiyama, A. Sakaue-Sawano, T. Iimura, K. Fukami, T. Kitaguchi, K. Kawakami, H. Okamoto, S.-i. Higashijima and A. Miyawaki, *Proc. Natl. Acad. Sci. U. S. A.*, 2009, **106**, 20812–20817.
- 27 P. D. S. Dong, C. A. Munson, W. Norton, C. Crosnier, X. Pan, Z. Gong, C. J. Neumann and D. Y. R. Stainier, *Nat. Genet.*, 2007, **39**, 397–402.
- 28 W. Denk, J. H. Strickler and W. W. Webb, *Science*, 1990, **248**, 73–76.
- 29 T.-H. Tsai, C.-Y. Lin, H.-J. Tsai, S.-Y. Chen, S.-P. Tai, K.-H. Lin and C.-K. Sun, *Opt. Lett.*, 2006, **31**, 930–932.
- 30 N. G. Gurskaya, A. F. Fradkov, A. Terskikh, M. V. Matz, Y. A. Labas, V. I. Martynov, Y. G. Yanushevich, K. A. Lukyanov and S. A. Lukyanov, *FEBS Lett.*, 2001, **507**, 16–20.
- 31 A. Miyawaki, J. Llopis, R. Heim, J. M. McCaffery, J. A. Adams, M. Ikura and R. Y. Tsien, *Nature*, 1997, **388**, 882–887.
- 32 A. Miyawaki, O. Griesbeck, R. Heim and R. Y. Tsien, *Proc. Natl. Acad. Sci. U. S. A.*, 1999, **96**, 2135–2140.
- 33 S. Higashijima, M. A. Masino, G. Mandel and J. R. Fetcho, *J. Neurophysiol.*, 2003, **90**, 3986–3997.
- 34 V. V. Belousov, A. F. Fradkov, K. A. Lukyanov, D. B. Staroverov, K. S. Shakhbazov, A. V. Terskikh and S. Lukyanov, *Nat. Methods*, 2006, **3**, 281–286.
- 35 P. Niethammer, C. Grabher, A. T. Look and T. J. Mitchison, *Nature*, 2009, **459**, 996–999.
- 36 B. W. Kusik, M. J. Carvan III and A. J. Udvardia, *Mar. Biotechnol.*, 2008, **10**, 750–757.
- 37 S. A. Farber, M. Pack, S.-Y. Ho, I. D. Johnson, D. S. Wagner, R. Dosch, M. C. Mullins, H. S. Hendrickson, E. K. Hendrickson and M. E. Halpern, *Science*, 2001, **292**, 1385–1388.
- 38 S. A. Carney, R. E. Peterson and W. Heideman, *Mol. Pharmacol.*, 2004, **66**, 512–521.
- 39 S. Park, M.-R. Lee and I. Shin, *Chem. Soc. Rev.*, 2008, **37**, 1579–1591.
- 40 S. T. Laughlin, J. M. Baskin, S. L. Amacher and C. R. Bertozzi, *Science*, 2008, **320**, 664–667.
- 41 X. Chen, S.-K. Ko, M. J. Kim, I. Shin and J. Yoon, *Chem. Commun.*, 2010, **46**, 2751–2753.
- 42 J. Li, H.-H. Ha, L. Guo, D. Coomber and Y.-T. Chang, *Chem. Commun.*, 2010, **46**, 2931–2934.
- 43 Y.-K. Yang, S.-K. Ko, I. Shin and J. Tae, *Nat. Protoc.*, 2007, **2**, 1740–1745.
- 44 Y.-K. Yang, S.-K. Ko, I. Shin and J. Tae, *Org. Biomol. Chem.*, 2009, **7**, 4590–4593.
- 45 X. Chen, K.-H. Baek, Y. Kim, S.-J. Kim, I. Shin and J. Yoon, *Tetrahedron*, 2010, **66**, 4016–4021.
- 46 M. Santra, D. Ryu, A. Chatterjee, S.-K. Ko, I. Shin and K. H. Ahn, *Chem. Commun.*, 2009, 2115–2117.
- 47 B. Tang, L. J. Cui, K. H. Xu, L. L. Tong, G. W. Yang and L. G. An, *ChemBioChem*, 2008, **9**, 1159–1164.
- 48 M. Korbas, S. R. Blechinger, P. H. Krone, I. J. Pickering and G. N. George, *Proc. Natl. Acad. Sci. U. S. A.*, 2008, **105**, 12108–12112.
- 49 F. Qian, C. Zhang, Y. Zhang, W. He, X. Gao, P. Hu and Z. Guo, *J. Am. Chem. Soc.*, 2009, **131**, 1460–1468.
- 50 Z. Xu, K.-H. Baek, H. N. Kim, J. Cui, X. Qian, D. R. Spring, I. Shin and J. Yoon, *J. Am. Chem. Soc.*, 2010, **132**, 601–610.
- 51 K. M. K. Swamy, S.-K. Ko, S. K. Kwon, H. N. Lee, C. Mao, J.-M. Kim, K.-H. Lee, J. Kim, I. Shin and J. Yoon, *Chem. Commun.*, 2008, 5915–5917.
- 52 S. Lepiller, V. Laurens, A. Bouchot, P. Herbomel, E. Solary and J. Chluba, *Free Radical Biol. Med.*, 2007, **43**, 619–627.
- 53 Y.-K. Yang, H. J. Cho, J. Lee, I. Shin and J. Tae, *Org. Lett.*, 2009, **11**, 859–861.
- 54 M. Santra, S.-K. Ko, I. Shin and K. H. Ahn, *Chem. Commun.*, 2010, **46**, 3964–3966.
- 55 P. Zrazhevskiy, M. Sena and X. Gao, *Chem. Soc. Rev.*, 2010, **39**, 4326–4354.
- 56 B. Dubertret, P. Skourides, D. J. Norris, V. Noireaux, A. H. Brivanlou and A. Libchaber, *Science*, 2002, **298**, 1759–1762.
- 57 S. Rieger, R. P. Kulkarni, D. Darcy, S. E. Fraser and R. W. Koster, *Dev. Dyn.*, 2005, **234**, 670–681.
- 58 S. W. Son, J. H. Kim, S. H. Kim, H. Kim, A.-Y. Chung, J. B. Choo, C. H. Oh and H.-C. Park, *Skin Res. Technol.*, 2009, **15**, 157–160.
- 59 M. Suzuki, Y. Husimi, H. Komatsu, K. Suzuki and K. T. Douglas, *J. Am. Chem. Soc.*, 2008, **130**, 5720–5725.